Decreased Levels of the RNA Splicing Factor Prpf3 in Mice and Zebrafish Do Not Cause Photoreceptor Degeneration

John J. Graziotto,[1,2] *Chris F. Inglehearn,*[3] *Michael A. Pack,*[4,5] *and Eric A. Pierce*[1]

Purpose. Pre-mRNA processing factor 3 (PRPF3) is a spliceosomal component essential for pre-mRNA processing. Mutations in *PRPF3* have been implicated in retinitis pigmentosa (RP) 18 through an unknown mechanism. The authors created and characterized *Prpf3* knockout mice and zebrafish to determine whether RP18 is a result of haploinsufficiency.

Methods. Mice were produced from a *Prpf3* gene trap cell line, and parameters of retinal function, structure, and RNA splicing were analyzed. The retinas of *prpf3* insertional mutant zebrafish were also analyzed histologically.

Results. Homozygous *Prpf3* knockout mice do not survive to 14 days postfertilization (dpf), implying that this allele is required for early embryonic development. Homozygous *Prpf3* knockout zebrafish die by 4dpf, well beyond the mid-blastula transition at which transcription activates. Zebrafish knockout embryos reveal abnormally high levels of cell death in the developing eye. Heterozygous *Prpf3* knockout mice have less than the expected 50% reduction in Prpf3 at the mRNA and protein levels, implying compensatory expression from the wild-type allele. The heterozygous mice develop normally, with no changes in retinal function, no evidence for photoreceptor degeneration at up to 23 months of age, and no decrease in pre-mRNA splicing of transcripts mutated in other forms of RP in the retina. Similarly, heterozygous *prpf3* knockout zebrafish develop normally and show no retinal degeneration up to 12 months of age.

Conclusions. These models suggest that RP18 is not a result of haploinsufficiency but instead arises from a toxic gain of function caused by missense mutations in *PRPF3*. (*Invest Ophthalmol Vis Sci.* 2008;49:3830–3838) DOI:10.1167/iovs.07-1483

A ubiquitous process in eukaryotic cells, pre-mRNA splicing is an essential step in gene expression. It takes place in a large ribonucleoprotein complex called the spliceosome, which, in addition to the pre-mRNA substrate, is composed of five small nuclear ribonucleoprotein complexes (snRNPs), U1, U2, U4/U6, and U5, and a host of non-snRNP accessory proteins (for reviews, see Krämer[1] and Krainer[2]).

Pre-mRNA processing factor 3 (PRPF3) protein is associated with the U4/U6 snRNP complex and is necessary for the integrity of the U4/U6/U5 tri-snRNP complex, without which splicing cannot occur.[3,4] The exact function of the PRPF3 protein is unknown, but several domains and interacting partners have been identified, including a direct interaction with the U4/U6 snRNP[5] and other spliceosomal proteins, among them PRPF4, cyclophilin H, hPRP6, and hSNU66.[6–9] The C terminus is the most highly conserved region of PRPF3, suggesting it has an important function.[3]

In recent years, two missense mutations in the highly conserved C terminus of PRPF3 and mutations in three other spliceosomal proteins have been implicated in autosomal dominant retinitis pigmentosa (adRP).[10] The other three retinitis pigmentosa (RP) genes encode PRPF8 and PRPF31, which are mutated in RP13 and RP11, respectively, and Pim-1–associated protein (PAP-1), which is mutated in RP9.[10–14]

Affecting approximately 1 in every 3000 people worldwide, RP is the most common inherited form of blindness.[15,16] RP patients experience progressive night blindness because of the loss of rod photoreceptor cells of the retina, followed by loss of peripheral vision and eventual blindness resulting from secondary degeneration of cones later in life.[17] RP is genetically heterogeneous and can be inherited by autosomal dominant (adRP), autosomal recessive (arRP), or X-linked (xlRP) transmission.[16] Despite this heterogeneity, most of the genes implicated in RP are expressed specifically in photoreceptor cells and encode proteins involved in the phototransduction cascade, photoreceptor structure, or other components of known visual pathways.[18] In all, mutations in 36 different genes have been shown to cause RP,[19] but the mechanisms by which defects in these genes lead to photoreceptor death are not understood.[18]

The discovery that 4 of the 14 known forms of dominant RP are caused by mutations in splicing factors suggests a novel and unexpected pathway to retinal degeneration. However, it is unclear how mutations in these ubiquitously expressed splicing factors lead to retina-specific disease. This question is of particular importance because, as a group, the RNA splicing factor forms of RP are the second most common cause of RP; the first is RP caused by mutations in rhodopsin.[20]

Several mechanisms may explain the specificity of the disease caused by the identified mutations in RNA splicing factors. Splicing factor RP could result from haploinsufficiency of functional splicing factors. The lack of a phenotype outside the eye could be attributed to the fact that photoreceptors are highly biosynthetically active, terminally differentiated cells that have a constant need to produce protein because of the shedding and replacement of outer segment discs.[21,22] Haploinsufficiency of splicing factors could therefore be particularly detrimental to photoreceptors, whereas other tissues and cell types function adequately with one working allele. A second hypoth-

From the [1]F. M. Kirby Center for Molecular Ophthalmology, Scheie Eye Institute, and the Departments of [2]Neuroscience, [4]Medicine, and [5]Cell and Developmental Biology, University of Pennsylvania School of Medicine, Philadelphia, Pennsylvania; and the [3]Section of Ophthalmology and Neuroscience, Leeds Institute of Molecular Medicine, University of Leeds, St. James's University Hospital, Leeds, United Kingdom.

Supported by Foundation Fighting Blindness, Research to Prevent Blindness, the Zeigler Foundation, the F. M. Kirby Foundation, the Mackall Foundation Trust, the Rosanne Silberman Foundation, and National Eye Institute Grant T32-EY-007035 (JJG).

Submitted for publication November 19, 2007; revised May 8, 2008; accepted July 17, 2008.

Disclosure: **J.J. Graziotto**, None; **C.F. Inglehearn**, None; **M.A. Pack**, None; **E.A. Pierce**, None

The publication costs of this article were defrayed in part by page charge payment. This article must therefore be marked "*advertisement*" in accordance with 18 U.S.C. §1734 solely to indicate this fact.

Corresponding author: Eric A. Pierce, F. M. Kirby Center for Molecular Ophthalmology, Scheie Eye Institute, University of Pennsylvania School of Medicine, 422 Curie Boulevard, Philadelphia, PA 19104; epierce@mail.med.upenn.edu.

Investigative Ophthalmology & Visual Science, September 2008, Vol. 49, No. 9

esis is that mutations in RP-related splicing factors disrupt the splicing of one or more retina-specific RNA species. This may occur through interaction of the RP splicing factors with as yet unidentified retina-specific splicing cofactors. The third hypothesis considers the possibility that the mutations confer a gain of function in the mutant splicing factors that is toxic in photoreceptors (for a review, see Mordes et al.[23]).

Most of what is known about PRPF3 and related splicing factors is derived from studies in yeast or in cell culture. Here we describe the development and characterization of *Prpf3* knockout mice and the characterization of *prpf3* insertional mutant zebrafish.[24] With the use of these two models, we determined that decreased levels of *Prpf3* do not cause differences in the structure or function of mouse or zebrafish retina, whereas the absence of *Prpf3* results in embryonic lethality in both animals.

Materials and Methods

Animals

This research was performed under the guidelines of and were approved by the Institutional Animal Care and Use Committee of the University of Pennsylvania (Philadelphia, PA) and conforms to the ARVO Statement for the Use of Animals in Ophthalmic and Vision Research. Wild-type C57BL/6J mice were obtained from Jackson Laboratories (Bar Harbor, ME).

Embryonic Stem Cell Culture

The gene trap mouse embryonic stem cell line RRO284 was obtained from BayGenomics (http://baygenomics.ucsf.edu/). On receipt, cells were thawed and cultured in embryonic stem cell medium (Dulbecco modified Eagle medium [DMEM; Gibco, Grand Island, NY]) with 15% fetal bovine serum (Hyclone, Logan, UT), 1% nonessential amino acids (Gibco), 0.1 mM β-mercaptoethanol (Sigma, St. Louis, MO), and 1250 U/mL leukemia inhibitory factor (Chemicon, Temecula, CA) on a primary mouse embryo fibroblast monolayer (Chemicon). G418-resistant clones were isolated and expanded for injection into blastocysts to produce chimeric mice.[25]

Production of Chimeric Mice

To produce chimeric mice, RRO284 embryonic stem cells were microinjected into C57Bl/6 blastocysts at the Chimeric and Transgenic Mouse Core Facility at the University of Pennsylvania School of Medicine. Highly chimeric founder mice were crossed with C57Bl/6 mice to generate heterozygous *Prpf3*$^{+/-}$ gene trap mice. Sibling crosses were performed to try to obtain homozygous *Prpf3*$^{-/-}$ mice.

Genotyping of Mice

Genotyping of the *Prpf3* mice was performed by Southern blotting and PCR. Southern blot analysis was also used to confirm the location of the gene trap allele and to screen for homozygous embryos. A number of probes were used for Southern blot analysis. Probe 1 was a 359-bp probe amplified from genomic DNA 5′ to the predicted location of the gene trap cassette in the *Prpf3* gene using the following primers: forward, EAP1590 5′ CAG GGG CTG AAG TTT GTG AGG TGA GTA G 3′; reverse, EAP1768 5′ GAA CGC TGT CTT CTG AAT GAG CAG G 3′. Probe 2 measured 328 bp and was amplified toward the 3′ end of the same *Bam*HI fragment using the following primers: forward, EAP2572 5′ TTT TAA TCT CTT GTC TTA TAG 3′; reverse, EAP2573 5′ AAG TTA GTA ATA TTC AAG TAA AT 3′. Probe 3 detects the next *Bam*HI fragment in the *Prpf3* gene and was amplified using (forward) EAP2574 5′ GCT CAA TTG GAG AAG CTG CAA GCA 3′ and (reverse) EAP2575 5′ GCA AGA TAA AAT AAG CCC TGG GTT CAT 3′ to yield a 398-bp probe. Probe 4 was against exon 16 in the last *Bam*HI fragment in the *Prpf3* gene using primers (forward) EAP2681 5′ CCG GAG CTT TGG AGA GAT GAA GTT TA 3′ and (reverse) EAP2682 5′ CTT TAA TCA TAT GCA CAT ACA GGA TGG A 3′ to yield a 320-bp probe. DNA from tail biopsy specimens or embryos was purified and digested with *Bam*HI and processed for Southern blot analysis with radiolabeled probes, as described.[26] For genotyping of mice by PCR, forward and reverse primers specific to the gene trap cassette were designed to amplify a 674-bp product to determine the presence or absence of the gene trap allele. The primers were (forward) EAP1668 5′ TCT ACT GCC CTT GGG ATC CTA CCG TTC 3′ and (reverse) EAP1669 5′ TGC CAG TTT GAG GGG ACG ACG ACA GTA TC 3′.

Northern Blotting

Four or more retinas of 4-week-old mice of each genotype were pooled and processed for Northern blotting using reagent (Trizol; Invitrogen, Carlsbad, CA). Total RNA (15–20 μg) was loaded per lane on a denaturing 0.8% agarose gel, transferred overnight to a nylon membrane (Schleicher & Schuell, Dassel, Germany), cross-linked, and stored or hybridized according to standard protocols.[27] A 652-bp radiolabeled probe against the mouse *Prpf3* transcript was amplified from cDNA using primers (forward) EAP1798 5′ CAG ATG ATG GAA GCA GCA ACA CGA C 3′ and (reverse) EAP1799 5′ TTC TAG CAG CTT GTG AAA TCT CT 3′. This probe spans exons 5 to 8 of the *Prpf3* transcript. To assess total RNA per lane, a probe against the housekeeping gene acidic ribosomal phosphoprotein P0 (36B4) was used.[28] Probes were hybridized to membranes overnight at 65°C, washed, and exposed to phosphor screens for detection. Phosphor screens were scanned with a phosphor imager and were quantified with appropriate software (ImageQuant 5.2; Molecular Dynamics, Sunnyvale, CA). Blots were stripped and reprobed several times.

Western Blotting

Retinas were solubilized by sonication in LDS sample buffer (Invitrogen), and 100 μg reduced protein was separated in each lane of a 3% to 8% Tris-acetate polyacrylamide gel (NuPage; Invitrogen). Proteins were transferred electrophoretically to polyvinylidene difluoride (PVDF) membrane (Invitrogen) and were blocked in 10% nonfat dry milk solution for 1 hour at room temperature. Primary antibodies against Prpf3 protein were a generous gift from James Hu.[8] Alkaline phosphatase–conjugated ant–rabbit secondary antibodies (Vector Laboratories, Burlingame, CA) were used in conjunction with ECF reagent (Amersham Pharmacia Biotech, Uppsala, Sweden), blots were scanned with a phosphor imager (Storm), and band intensities were quantified (ImageQuant 5.2; Molecular Dynamics).

Electroretinographic Analysis

Electroretinography was performed as previously described.[29] Briefly, full-field electroretinograms were recorded in a ganzfeld on dark-adapted, anesthetized mice taking care to maintain 37°C body temperature at all times. Pupils were dilated with 1% tropicamide. Retinal responses were detected with platinum electrodes embedded in contact lenses contacting the cornea and were recorded using custom software.

Light and Electron Microscopy

Preparation of retinas for light and electron microscopy was performed as previously described.[30] For histologic analysis of the retina and other tissues, animals were killed and perfused with 4% paraformaldehyde in phosphate-buffered saline (PBS; Electron Microscopy Sciences). Eyes were enucleated and, after removal of the cornea and lens, were fixed for an additional 2 to 3 hours at 4°C. Tissue was then transferred to 30% sucrose solution in PBS, incubated overnight at 4°C, and embedded and frozen in OCT (Triangle Biomedical Sciences) for cryosectioning. Ten-micrometer–thick sections were cut, mounted onto slides (Superfrost Plus; Fisher Scientific, Pittsburgh, PA), and stained with alkaline toluidine blue for light microscopy. For electron microscopy, perfused eyecups were transferred to 2% paraformaldehyde + 2% glutaraldehyde in 0.2 M sodium cacodylate buffer (pH 7.4) for 4 hours and then cut into 2-mm pieces. These were postfixed in 1% OsO_4 and were stained with 1% uranyl acetate, dehy-

drated, and embedded (EMbed812; Electron Microscopy Sciences). One-micrometer–thick sections were then cut and stained with alkaline toluidine blue for light microscopy, and 60- to 80-nM ultrathin sections were stained with lead citrate/uranyl acetate and examined using a transmission electron microscope (FEI Tecnai).

Zebrafish Maintenance and Breeding

Maintenance of the zebrafish colony is described in detail elsewhere.[31,32] Heterozygous *prpf3*^{hi2791Tg} were obtained from Nancy Hopkins[24] and were outcrossed onto the Tupfel long-fin wild-type strain. Fish identified as heterozygous (*prpf3*$^{+/-}$) for the mutation by PCR assay were intercrossed to produce homozygous (*prpf3*$^{-/-}$) zebrafish. Mutant fish were identified by multiplex PCR assay of DNA from tailfin biopsy using the following primers: EAP1961, 5′ GGG TGC AGT GAA GTC CAG ATA C 3′; EAP1962, 5′ CGT TGC AAA CCA ACT GAA TCC C 3′; EAP1963, 5′ GTT CCT TGG GAG GGT CTC CTC 3′. Embryos were grown in 10-cm dishes in E3 media supplemented with 0.6 μM methylene blue (Fisher Scientific) at 28.5°C. Embryos or adult zebrafish of various ages were fixed and processed for light microscopy or histochemistry, as described. The zebrafish *prpf3* Northern probe was amplified from zebrafish cDNA using the following primers: EAP2350, 5′ TTC GGC AAG CAG TTT CGT TGA GCG TCT GTT 3′; EAP2351, 5′ CAC CCC CTG CTT GGT TCA TAG ATC GTG GAG 3′.

Results

Generation of *Prpf3* Knockout Mice

To generate *Prpf3* knockout mice, we obtained the *Prpf3* gene trap cell line RRO284 from the BayGenomics gene trap Consortium (http://baygenomics.ucsf.edu/). Based on 5′ RACE, this cell line contains the pGT2lxf gene trap vector inserted after exon 2 of Prpf3 (Fig. 1). We expanded these cells in selective media and chose a clone for injection into blastocysts to produce chimeric mice. Resultant chimeras were outcrossed to obtain germ line transmission of the gene trap allele. The location of the gene trap cassette in the mouse genome was verified by Southern blot analysis (Figs. 1D, 1F–I) As shown in Figure 1, probes at the 5′ and 3′ ends of the *Prpf3* gene detected the insertion of the gene trap vector, whereas probes in the middle of the *Prpf3* gene showed diminished signals. These results indicate that the insertion of the gene trap vector was associated with a deletion of a significant portion (exons 3–14) of the *Prpf3* gene.

Mice heterozygous for the gene trap allele (*Prpf3*$^{+/-}$) were healthy and fertile and had no developmental defects. Intercrosses of *Prpf3*$^{+/-}$ mice have not generated any homozygous *Prpf3* knockout mice (*Prpf3*$^{-/-}$) to date. Southern blot analysis of 34 embryos yielded 28 *Prpf3*$^{+/-}$, 6 *Prpf3*$^{+/+}$, and zero *Prpf3*$^{-/-}$ genotypes, showing that *Prpf3*$^{-/-}$ embryos die before embryonic day 14. Ten examples are shown in Figure 1E–I. The presence of the gene trap cassette in heterozygous mice (*Prpf3*$^{+/-}$) was tracked by PCR assay (Fig. 1E), which correlated perfectly with the results of the Southern analyses.

Expression of *Prpf3* in Wild-Type and Mutant Animals

Prpf3 is known to be expressed in many tissues,[10] but protein expression levels in different tissues have not been directly compared. We compared the expression levels of Prpf3 in retina, brain, liver, spleen, kidney, intestine, lung, testis, and heart (Fig. 2A) and found that the levels of Prpf3 protein varied greatly between tissues, with the highest levels in the testis and the next highest in the retina. The level of Prpf3 in the heart was approximately 75% of that detected in retina; in brain, liver, lung, and spleen, the levels were approximately 50% of the amount found in the retina.

To determine whether the presence of the gene trap vector decreased the level of *Prpf3* transcript in our mutant mice, we performed Northern blot analysis on retinal RNA from young (4-week-old) mice using radiolabeled probes against *Prpf3* and a loading control (Fig 2B). After normalizing the *Prpf3* signal to the loading control, a 37% (±19%) (n = 5; t-test = 0.01) reduction of *Prpf3* transcript was observed in the *Prpf3*$^{+/-}$ mice compared with *Prpf3*$^{+/+}$ mice.

Similarly, we measured the expression levels of Prpf3 protein in the retinas of the *Prpf3*$^{+/-}$ mice using Western blotting (Fig 2C). The 77-kDa Prpf3 band was reduced by 27.5% (±10.1%; n = 3; t-test = 0.04) in *Prpf3*$^{+/-}$ compared with *Prpf3*$^{+/+}$ mice. Similar results were obtained with several anti–Prpf3 antibodies (data not shown).

Pre-mRNA Splicing

We reasoned that if an optimal level of *Prpf3* was essential to sustain levels of spliced RNA for abundant transcripts in the retina, we should see lower levels of highly expressed transcripts, such as rhodopsin, when less Prpf3 is present in the retina. We also reasoned that the same could apply to mRNA transcripts for other proteins implicated in RP. We tested this hypothesis by evaluating the levels and sizes of several RP disease gene transcripts in retinal RNA from *Prpf3*$^{+/-}$ and control mice by Northern blot analysis. The mRNAs evaluated include those for rhodopsin (*Rho*), rod cGMP-gated channel alpha subunit (*Cnga1*), ATP-binding cassette transporter (*Abca4*), neural retina leucine zipper (*Nrl*), rod cGMP phosphodiesterase beta subunit (*Pde6b*), and retinaldehyde-binding protein 1 (*Rlbp1*). No differences in the size or amount of any of these transcripts were detected between retinal RNA from *Prpf3*$^{+/-}$ or control mice (Fig. 3). Even rhodopsin, which is the most abundant transcript in retina, is present at normal levels in the *Prpf3*$^{+/-}$ mouse retina, indicating that processing of this transcript is not limited by the decreased levels of *Prpf3*.

Retinal Function

We used electroretinography to measure the retinal function of *Prpf3*$^{+/-}$ mice at 9, 18, and 23 months of age. For these analyses, we recorded scotopic a-waves and b-waves (Fig. 4A) to assess rod photoreceptor and bipolar function and photopic b-waves (Fig. 4B) to assess cone responses. All recordings were carried out on dark-adapted *Prpf3*$^{+/-}$ and littermate *Prpf3*$^{+/+}$ control mice. No significant differences were found between heterozygous *Prpf3*$^{+/-}$ and littermate control *Prpf3*$^{+/+}$ mice at any time up to 23 months of age (Fig. 4). Representative scotopic traces of 23-month-old *Prpf3*$^{+/+}$ and *Prpf3*$^{+/-}$ mice are shown in Figure 4C.

Retinal Morphology and Ultrastructure

Light microscopic analyses showed that the retinal morphology in *Prpf3*$^{+/-}$ mice was normal at all ages tested, including 9 and 23 months (Fig. 5A–D). The outer nuclear layer was of normal thickness, with 10 layers of nuclei present in *Prpf3*$^{+/+}$ and *Prpf3*$^{+/-}$ mice. The outer segments of the rod photoreceptors were of normal length, and the RPE was intact. The inner nuclear layer also appeared to be normal.

The ultrastructure of the RPE and photoreceptors in *Prpf3*$^{+/-}$ mice was also normal (Figs. 5E–L). The RPE-photoreceptor interface was comparable between *Prpf3*$^{+/+}$ and *Prpf3*$^{+/-}$ mice (Figs. 5E, 5I), the outer segment discs were stacked in an orderly fashion along the length of the photoreceptors (Figs. 5F, 5J), the inner segments appeared healthy and have normal numbers of mitochondria (Figs. 5G, 5K), and the outer nuclear layer nuclei were comparable between the two groups (Figs. 5H, 5L).

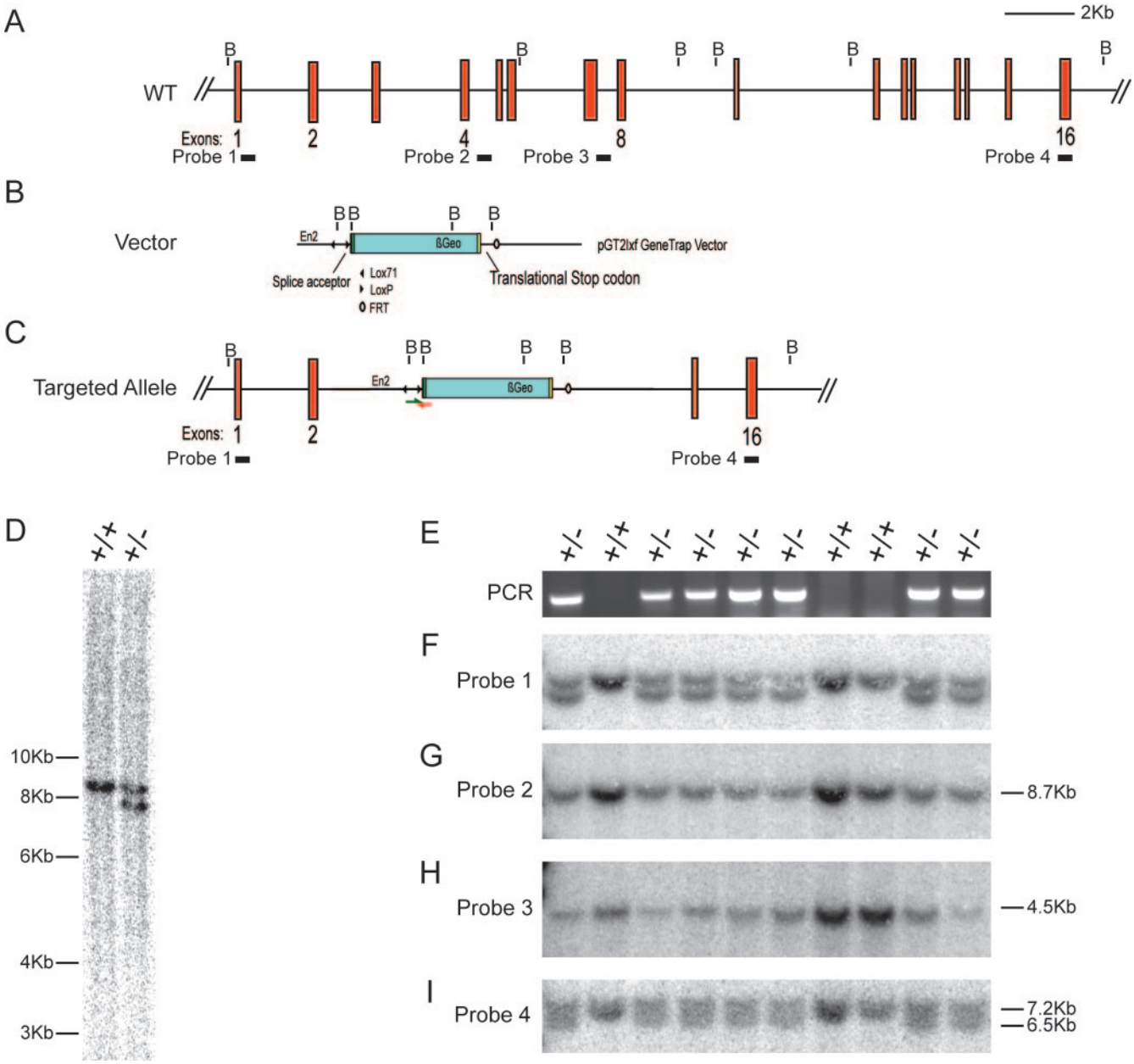

FIGURE 1. Production of *Prpf3* knockout mice. (**A**) The 16-exon wild-type (WT) allele of *Prpf3* gene. *Bam*HI restriction digest sites are designated B. (**B**) The pGT2lxf gene trap vector. The vector has a splice acceptor sequence at the 5′ end, followed by a β-galactosidase/neomycin resistance fusion cassette (BGeo) ending in a translational stop codon. (**C**) The gene trap version of the *Prpf3* gene consists of exons 1 and 2, followed by the gene trap vector, which caused a large deletion of the *Prpf3* gene when it inserted, as indicated by the results of Southern blot analyses with probes 2, 3, and 4. (**D**) Southern blotting using the probe indicated in (**C**) showing the 8.6-kb wild-type band, and both the 8.6-kb wild-type and the smaller mutant band in heterozygous knockout mouse DNA. (**E**) Gene trap alleles are detectable with a PCR-based assay. Shown are 10 reactions using DNA from E14 mice and primers indicated in (**C**) showing perfect correlation with the Southern blot results in (**F–I**). (**F–I**) Sample Southern blots of E14 mice. Shown are 10 of 34 mice from +/− intercrosses. No $Prpf3^{-/-}$ mice were obtained to date. (**G**) Probe 2 shows a decrease in signal intensity in +/− mice compared with +/+ mice but no size change, indicating that this part of the *Prpf3* gene has been deleted in the mutant allele. (**H**) Probe 3 shows similar results to probe 2, indicating that this downstream portion of the *Prpf3* gene is also deleted in the mutant allele. (**I**) Probe 4 shows a size change in +/− mice compared with +/+, indicating this fragment contains the 3′ end of the gene trap vector. In sum, the Southern blot results indicate that the region of *Prpf3* between exons 2 and 15 has been deleted in the mutant allele.

Mutant *Prpf3* Zebrafish

To study the effect of *Prpf3* deficiency in another model system, we obtained the *prpf3* insertional mutant zebrafish line $prpf3^{hi2791Tg}$ as a gift from Nancy Hopkins.[24] The mutant fish were outcrossed onto the Tupfel long-fin wild-type strain, and fish identified as heterozygous ($prpf3^{+/-}$) for the mutation by PCR assay were intercrossed. We verified that *prpf3* expression was decreased by Northern blot analysis of $prpf3^{+/+}$ compared with $prpf3^{+/-}$ fish using a probe against zebrafish *prpf3*. A decrease of approximately 40% in the *prpf3* transcript can be seen in the $prpf3^{+/-}$ lane compared with the wild-type lane using the 18S and 24S bands as loading controls (Fig. 6A). Homozygous $prpf3^{-/-}$ fish exhibited decreased head size and curled bodies and died by 4 days postfertilization (dpf), as described previously[24] (Figs. 6B, 6C). Microscopic analyses of

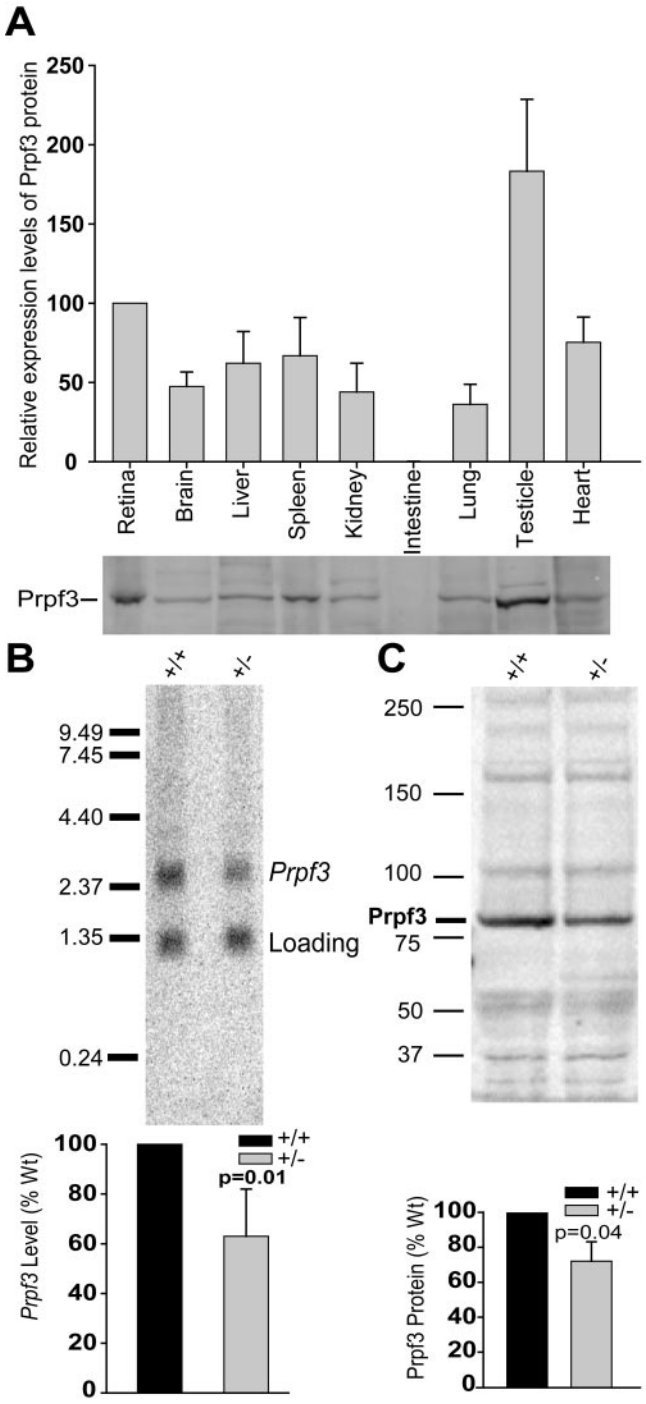

FIGURE 2. Expression of *Prpf3* transcript and protein. (**A**) Western blot analysis of equivalent amounts of total protein from various mouse tissue lysates with antibodies against Prpf3. The highest expression is found in the testis, followed by retina, spleen, and heart. Levels in other tissues are at least half those seen in the retina (values plotted normalized to retina). (**B**) Northern blot analysis of retinas of *Prpf3* mutant mice at postnatal day (P) 28. *Prpf3* levels in $Prpf3^{+/-}$ retina were reduced 37% (±19%; $n = 5$; *t*-test = 0.01) compared with wild-type retina. (**C**) Western blotting of Prpf3 protein. Retinal protein (150 μg) was blotted using antibodies against Prpf3. The 77-kDa Prpf3 band was reduced 27.5% (±10.1%; $n = 3$; *t*-test = 0.04) in the heterozygous animals compared with wild-type littermate controls.

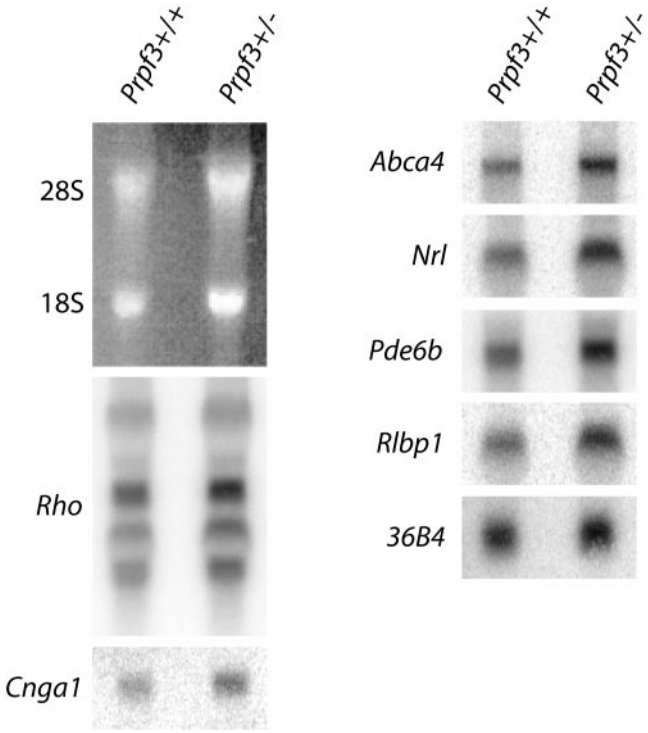

FIGURE 3. Pre-mRNA splicing. We directly compared mRNAs from $Prpf3^{+/+}$ and $Prpf3^{+/-}$ mouse retinas to look for alterations in splicing efficiency. We analyzed the amount of rhodopsin and several other RP disease gene transcripts using Northern blotting. As loading control, the 28S and 18S bands are shown, as is the 36B4 probe. No difference in the size or amount of any transcript examined has been found to date. *Rho*, rhodopsin; *Cnga1*, rod cGMP-gated channel alpha subunit; *Abca4*, ATP-binding cassette transporter; *Nrl*, neural retina leucine zipper; *Pde6b*, rod cGMP phosphodiesterase beta subunit; *Rlbp1*, retinaldehyde binding protein 1.

retinal structure at 2dpf showed that the $prpf3^{+/+}$ fish had more advanced retinal development than the $prpf3^{-/-}$ fish at this age (Figs. 6D, 6E). The wild-type retinas had the beginnings of laminae at this time, whereas the $prpf3^{-/-}$ retinas had many pyknotic nuclei. No differences in retinal structure were detected in the $prpf3^{+/-}$ fish at 4 days or 12 months of age (Figs. 6F–I). For example, at 12 months of age, normal amounts of rod and cone photoreceptor nuclei were present in the $prpf3^{+/-}$ retinas (Figs. 6H, 6I).

DISCUSSION

The results described here show that complete lack of *Prpf3* resulted in embryonic lethality in mice and zebrafish, demonstrating that Prpf3 is required for the viability of fish and mammals. The retinas of 2dpf homozygous $prpf3^{-/-}$ zebrafish demonstrated delayed retinal development and extensive cell death, suggesting that prpf3 plays an especially important role in this tissue. Prpf3 expression is highest in testis and retina, consistent with this idea. In contrast to the homozygotes, heterozygote knockout animals are phenotypically normal, with no changes in splicing noted and no evidence of photoreceptor degeneration or other abnormalities. These observations may be a consequence of compensation by the normal allele in heterozygous animals, suggesting the existence of a feedback mechanism for the expression of Prpf3. These results suggest that the T494M and P493S mutations in *PRPF3*, which cause the retinal degeneration RP18, alter rather than prevent

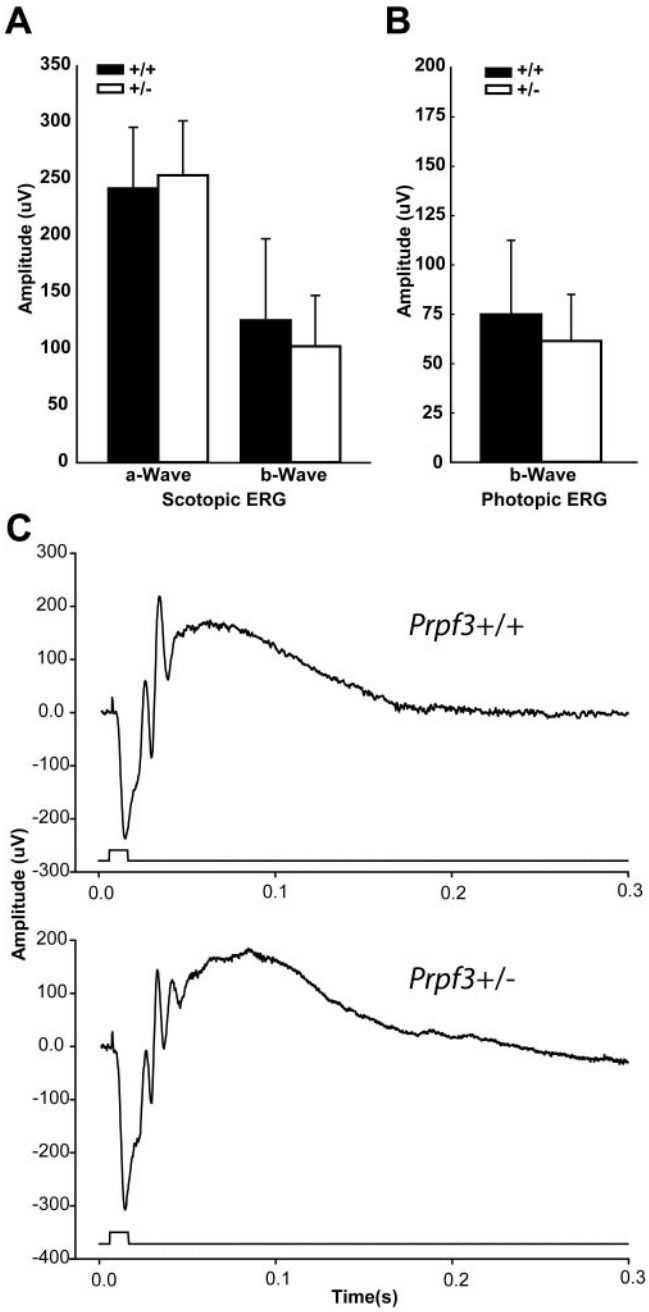

FIGURE 4. Retinal function. Electroretinography was performed on knockout mice at 23 months to assess retinal function. (**A**) Average scotopic a-wave and b-wave amplitudes are shown for wild-type (+/+) and littermate heterozygous knockout (+/−) mice. No significant differences were found up to 23 months of age ($Prpf3^{+/-}$, $n = 6$; $Prpf3^{+/+}$, $n = 7$; a-wave *t*-test = 0.68; b-wave *t*-test = 0.50). (**B**) Average photopic ERG amplitudes also show no alterations in cone function at 23 months of age ($Prpf3^{+/-}$, $n = 6$; $Prpf3^{+/+}$, $n = 7$; *t*-test = 0.45). (**C**) Representative scotopic traces at 23 months for $Prpf3^{+/+}$ and $Prpf3^{+/-}$ mice.

the function of *PRPF3,* and they indicate that haploinsufficiency is not the disease mechanism for RP18.

The Prpf3 protein has long been known to be essential for spliceosome integrity in yeast, and it is required for RNA splicing to occur.[4] Here we show that the Prpf3 protein is also essential for life in vertebrates. The *Prpf3* gene trap mice are homozygous embryonic lethal before embryonic day 14, demonstrating that Prpf3 is important at very early stages of development. This finding is comparable to several other splicing factor knockout mice that die early in development.[33–37] The zebrafish knockout model confirms this, with death by 4dpf. We presume that in both the $Prpf3^{-/-}$ mice and the zebrafish, embryonic death resulted from a lack of spliced RNA transcripts. Although transcription is activated starting at 3 hours after fertilization in zebrafish embryos, the survival of the $prpf3^{-/-}$ fish to 4dpf is not surprising because maternal mRNA and protein contribute to development for several days.[38–40]

The use of the mutant zebrafish was valuable because it allowed for evaluation of early retinal development in homozygous $prpf3^{-/-}$ fish. At 2dpf, the $prpf3^{-/-}$ fish demonstrated defects in retinal development, with less organized retinal layers than control fish (Fig. 6). The disorganization of the $prpf3^{-/-}$ retinas might have resulted from the widespread cell death seen in the retina. The fact that the eyes are not as well developed supports the hypothesis that Prpf3 is especially important for the growth and maintenance of this tissue. Indeed, our analysis shows that there is more Prpf3 protein in the retina than all other organs tested except for the testis, underscoring its importance for retinal maintenance.

It is possible that the abundance of Prpf3 protein in the retina partially explains the retina-specific phenotype observed in persons with mutations in the *PRPF3* gene. The flaw in this argument, however, is that male $Prpf3^{+/-}$ mice do not appear to have any alterations in testis structure (data not shown) and are fertile. Similarly, men with RP18 disease have not been reported to have defects in fertility.[41]

The extent of the decreased expression of *Prpf3* in the heterozygous knockout mice is approximately 30%, indicating compensation from the normal allele. This is a common finding among animals hemizygous for essential genes and can occur at both the mRNA and the protein levels.[42,43] The mechanisms for this compensation are thought to include increased transcription or translation of the remaining allele or decreased degradation of transcript or protein, implying the existence of a feedback regulatory mechanism for the expression of *Prpf3*.

The decrease in *Prpf3* expression observed in the $Prpf3^{+/-}$ mice is consistent and reproducible at the RNA and the protein levels. Despite the decrease in Prpf3, our data show that the mouse retina remains able to efficiently splice mRNA. We show that the splicing of the most abundant RNA transcript in the retina, rhodopsin, does not appear to be altered in heterozygous knockout mice. This is in contrast to at least one study of mutant *Prpf31*, which was found to inhibit splicing of Rhodopsin minigenes and to reduce rhodopsin expression in cell culture.[44] Similar results were obtained for the mRNAs from several other retinal disease genes, suggesting that the availability of the Prpf3 protein in the retina is not rate limiting for RNA splicing.

Mice expressing decreased levels of Prpf3 protein do not show retinal degeneration or any other functional phenotype at ages up to 2 years. Several hypotheses explain why decreased levels of Prpf3 do not lead to a degenerative phenotype. One is that the two mutations found in RP18 patients are not loss-of-function mutants but rather lead to a toxic gain of function. Two observations support this hypothesis. One is that there is no evidence for incomplete penetrance of RP18 among patients.[10,20,45] The second is the observation that homozygous *Prpf3*-T494M knockin mice are viable (Graziotto JJ, et al. *IOVS* 2006;47:ARVO E-Abstract 4588). If the T494M mutation did result in nonfunctional protein, we would have expected that mice homozygous for the *Prpf3*-T494M knockin mutation would also die in utero. Another possibility is compensation by other splicing factors that perform similar functions in the mouse retina. Multiple examples of functional redundancy can be seen in mouse models. For instance, mutations in the doublecortin gene in humans lead to severe defects

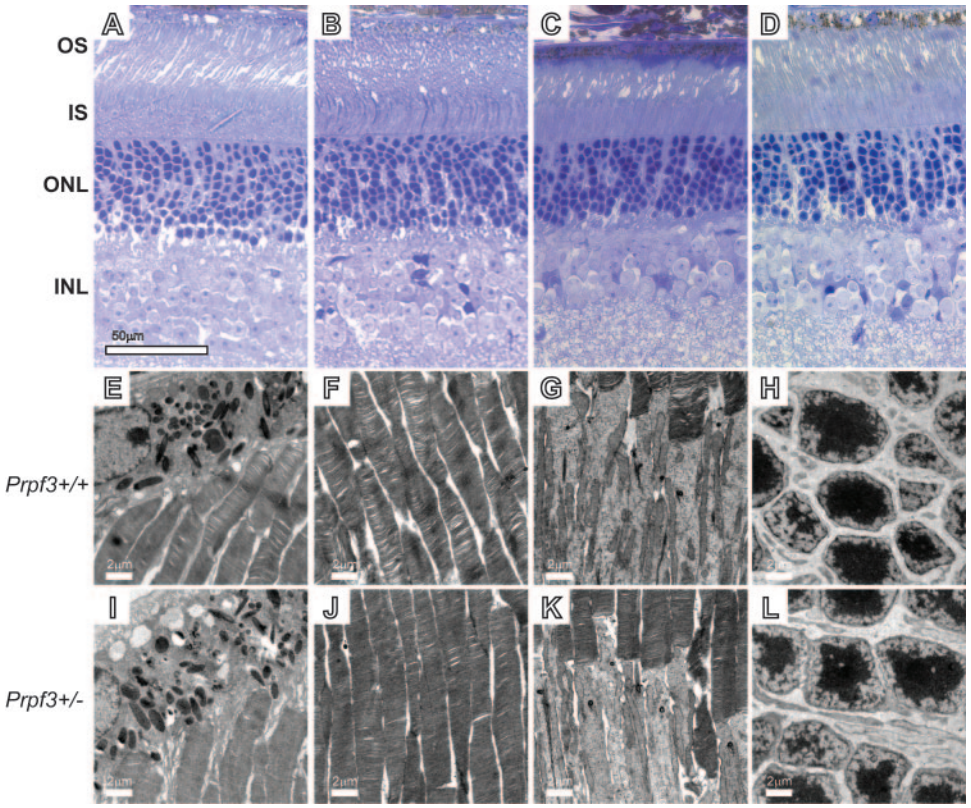

FIGURE 5. Histology and electron microscopy (EM) of retina. Thick plastic sections stained with toluidine blue reveal normal ONL layers at 9 (**A**, **B**) and 23 (**C**, **D**) months in *Prpf3*$^{+/+}$ (**A**, **C**) and *Prpf3*$^{+/-}$ (**B**, **D**) retinas (scale bar, 50 μm [**A–D**]). Outer segments also appear normal in length and density. Uranyl acetate–stained EM images reveal normal RPE-photoreceptor interface (**E**, **I**) Photoreceptor outer segments (**F**, **J**), inner segments (**G**, **K**), and photoreceptor nuclei (**H**, **L**) in *Prpf3*$^{+/+}$ (**E–H**) and *Prpf3*$^{+/-}$ (**I–L**) mice. OS, outer segment; IS, inner segment; ONL, outer nuclear layer; INL, inner nuclear layer.

in hippocampal development. In mice, however, doublecortin and doublecortin-like kinase 1 must be knocked out before a similar effect is seen, indicating partial redundancy of these two genes.[46] A third possibility is that biological differences between the mouse eye and the human eye make it difficult to model splicing factor RP in mice. For instance, mice have a much shorter lifespan than humans and live to only approximately 2 years of age, yet vertebrate photoreceptor outer

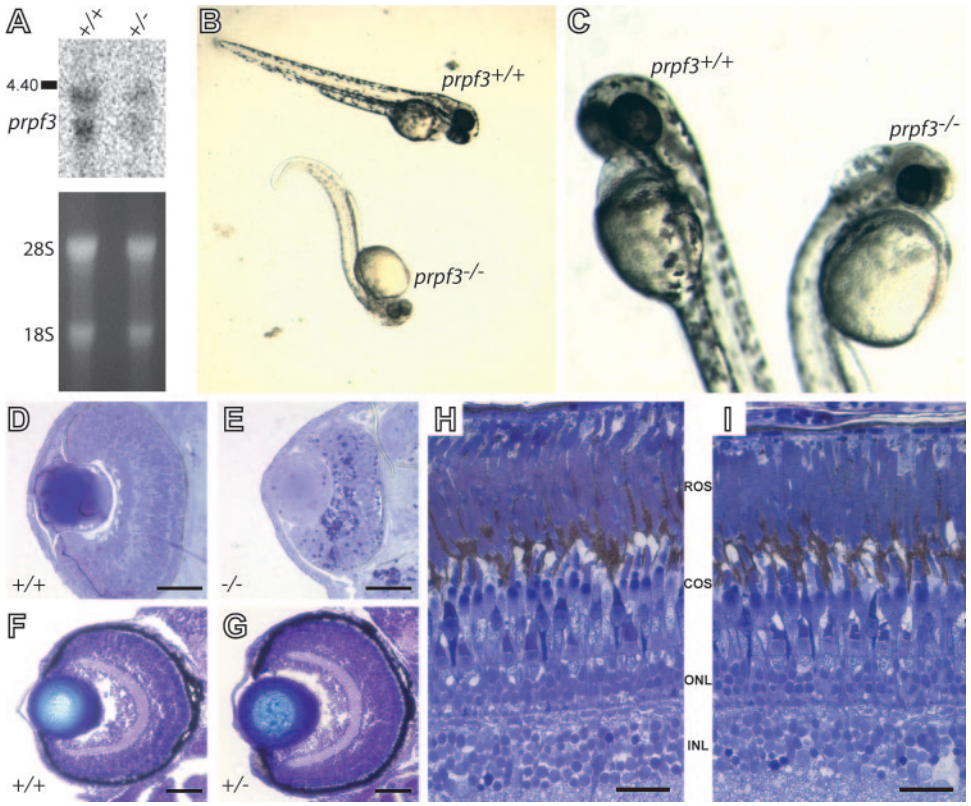

FIGURE 6. Mutant *prpf3* zebrafish. *prpf3*$^{+/-}$ zebrafish were obtained and intercrossed. (**A**) Northern blot of *prpf3* shows decreased levels of *prpf3* in *prpf3*$^{+/-}$ zebrafish compared with wild-type controls. 18S and 24S bands are shown for loading comparison. (**B**) *prpf3*$^{-/-}$ knockout zebrafish (*bottom*) are underdeveloped and have less pigmentation at 2 dpf than wild-type controls. (**C**) Homozygous *prpf3*$^{-/-}$ fish (*right*) have decreased head and eye size at 2dpf compared with *prpf3*$^{+/+}$ or *prpf3*$^{+/-}$ zebrafish (*left*). (**D**) Cross-section of wild-type 2dpf zebrafish eye at 40× magnification shows retinal lamina beginning to form. (**E**) Cross-section of *prpf3*$^{-/-}$ eye at 40× magnification shows underdeveloped retina and lens and dark-staining pyknotic nuclei. (**F**) 4dpf *prpf3*$^{+/+}$ 20× magnification zebrafish retina. (**G**) 4dpf *prpf3*$^{+/-}$ 20× magnification zebrafish retina. (**H**) One-year-old adult *prpf3*$^{+/+}$ zebrafish retina. (**I**) One-year-old adult *prpf3*$^{+/-}$ zebrafish retina. Scale bars, 50 μm. ROS, outer segments; COS, cone outer segments; ONL, outer nuclear layer; INL, inner nuclear layer.

segments turn over at a similar rate—every 9 to 12 days—in both.[47,48] At this rate, a mouse photoreceptor nearing the end of its 2-year lifespan will have completely turned over its outer segment approximately 70 times, but a human photoreceptor aged 20 years will have completed this process 700 times. Therefore, in absolute terms, mice may not live long enough for a given photoreceptor disease process to mimic the human form.

The gene trap approach for the generation of knockout mice, combined with the international consortia developed to characterize and archive the resultant embryonic stem cell lines, has clearly created a valuable resource for biomedical research.[49] Not all gene trap mouse lines, however, develop a phenotype. For instance, a recent study involving a gene trap *Mhy9* allele, a gene involved in inherited hearing loss, found that despite 50% less mRNA of *Mhy9* in heterozygotes, no hearing phenotype could be found, whereas homozygotes were embryonic lethal.[50] Therefore, conditional targeting techniques may be needed to obtain a homozygous knockout phenotype in a specific tissue in which the germ line knockout mutation is lethal in early embryos. However, given the essential nature of *Prpf3* for cell viability, *Prpf3* conditional knockout mice may not offer any further insight into RP18 because the photoreceptors that lack *Prpf3* would die in the complete absence of Prpf3 protein, a mechanism our observations suggest is not the underlying cause of RP18. Consistent with this idea, knocking *Prpf3* down in ARPE-19 or HeLa cells results in 50% loss of cells by 4 days and 90% cell death by 8 days after transfection relative to cells transduced with control vector.[51] Recent evidence also indicates that mutant forms of Prpf3, when overexpressed, may form aggregates under some conditions, potentially reinforcing the idea that the mutations are toxic.[52]

In conclusion, these studies suggest that though Prpf3 is developmentally important in vertebrates, it plays an especially important role in retina, which is evident from the increased retinal cell death in the zebrafish mutants. The high level of expression in this tissue supports this idea and may be directly related to the disease mechanism of RP18, but through a toxic effect of the T494M and P493S mutations rather than through haploinsufficiency. This is consistent with the dominant nature of disease inheritance. Future studies should therefore focus on the effects these two mutations have on pre-mRNA processing or of the behavior of Prpf3 in the retina. Information gained from these studies could have direct relevance for designing therapies for RP18 and other splicing factor forms of RP.

Acknowledgments

The authors thank James Hu for providing the antibody for Prpf3 used in this work and Nancy Hopkins for providing the mutant zebrafish line.

References

1. Krämer A. The structure and function of proteins involved in mammalian pre-mRNA splicing. *Annu Rev Biochem*. 1996;65:367–409.
2. Krainer AR. *Eukaryotic mRNA Processing*. New York: Oxford University Press; 1997.
3. Lauber J, Plessel G, Prehn S, et al. The human U4/U6 snRNP contains 60 and 90kD proteins that are structurally homologous to the yeast splicing factors Prp4p and Prp3p. *RNA*. 1997;3:926–941.
4. Anthony JG, Weidenhammer EM, Woolford JL Jr. The yeast Prp3 protein is a U4/U6 snRNP protein necessary for integrity of the U4/U6 snRNP and the U4/U6.U5 tri-snRNP. *RNA*. 1997;3:1143–1152.
5. Nottrott S, Urlaub H, Luhrmann R. Hierarchical, clustered protein interactions with U4/U6 snRNA: a biochemical role for U4/U6 proteins. *EMBO J*. 2002;21:5527–5538.
6. Horowitz DS, Kobayashi R, Krainer AR. A new cyclophilin and the human homologues of yeast Prp3 and Prp4 form a complex associated with U4/U6 snRNPs. *RNA*. 1997;3:1374–1387.
7. Teigelkamp S, Achsel T, Mundt C, et al. The 20kD protein of human [U4/U6.U5] tri-snRNPs is a novel cyclophilin that forms a complex with the U4/U6-specific 60kD and 90kD proteins. *RNA*. 1998;4:127–141.
8. Gonzalez-Santos JM, Wang A, Jones J, Ushida C, Liu J, Hu J. Central region of the human splicing factor Hprp3p interacts with Hprp4p. *J Biol Chem*. 2002;277:23764–23772.
9. Liu S, Rauhut R, Vornlocher HP, Luhrmann R. The network of protein-protein interactions within the human U4/U6.U5 tri-snRNP. *RNA*. 2006;12:1418–1430.
10. Chakarova CF, Hims MM, Bolz H, et al. Mutations in HPRP3, a third member of pre-mRNA splicing factor genes, implicated in autosomal dominant retinitis pigmentosa. *Hum Mol Genet*. 2002;11:87–92.
11. McKie AB, McHale JC, Keen TJ, et al. Mutations in the pre-mRNA splicing factor gene PRPC8 in autosomal dominant retinitis pigmentosa (RP13). *Hum Mol Genet*. 2001;10:1555–1562.
12. Vithana EN, Abu-Safieh L, Allen MJ, et al. A human homolog of yeast pre-mRNA splicing gene, PRP31, underlies autosomal dominant retinitis pigmentosa on chromosome 19q13.4 (RP11). *Mol Cell*. 2001;8:375–381.
13. Keen TJ, Hims MM, McKie AB, et al. Mutations in a protein target of the Pim-1 kinase associated with the RP9 form of autosomal dominant retinitis pigmentosa. *Eur J Hum Genet*. 2002;10:245–249.
14. Maita H, Kitaura H, Keen TJ, Inglehearn CF, Ariga H, Iguchi-Ariga SM. PAP-1, the mutated gene underlying the RP9 form of dominant retinitis pigmentosa, is a splicing factor. *Exp Cell Res*. 2004;300:283–296.
15. Berson EL. Retinitis pigmentosa: unfolding its mystery (review). *Proc Natl Acad Sci U S A*. 1996;93:4526–4528.
16. Bunker CH, Berson EL, Bromley WC, Hayes RP, Roderick TH. Prevalence of retinitis pigmentosa in Maine. *Am J Ophthalmol*. 1984;97:357–365.
17. Berson EL. Retinitis pigmentosa: the Friedenwald Lecture (review). *Invest Ophthalmol Vis Sci*. 1993;34:1659–1676.
18. Pierce EA. Pathways to photoreceptor cell death in inherited retinal degenerations. *Bioessays*. 2001;23:605–618.
19. RetNet. Retinal Information Network. http://www.sph.uth.tmc.edu/Retnet/; 2008. Accessed June 26, 2008.
20. Sullivan LS, Bowne SJ, Birch DG, et al. Prevalence of disease-causing mutations in families with autosomal dominant retinitis pigmentosa: a screen of known genes in 200 families. *Invest Ophthalmol Vis Sci*. 2006;47:3052–3064.
21. Anderson DH, Fisher SK, Steinberg RH. Mammalian cones: disc shedding, phagocytosis, and renewal. *Invest Ophthalmol Vis Sci*. 1978;17:117–133.
22. Anderson DH, Fisher SK. Disc shedding in rodlike and conelike photoreceptors of tree squirrels. *Science*. 1975;187:953–955.
23. Mordes D, Luo X, Kar A, et al. Pre-mRNA splicing and retinitis pigmentosa. *Mol Vis*. 2006;12:1259–1271.
24. Amsterdam A, Nissen RM, Sun Z, Swindell EC, Farrington S, Hopkins N. Identification of 315 genes essential for early zebrafish development. *Proc Natl Acad Sci U S A*. 2004;101:12792–12797.
25. Nagy A. *Manipulating the Mouse Embryo: A Laboratory Manual*. 3rd ed. Cold Spring Harbor, NY: Cold Spring Harbor Laboratory Press; 2003.
26. Ausubel FM, Brent R, Kingston RE, et al. *Current Protocols in Molecular Biology*. New York: John Wiley & Sons; 1994.
27. Sambrook J, Fritsch EF, Maniatis T. *Molecular Cloning: A Laboratory Manual*. Cold Spring Harbor, NY: Cold Spring Harbor Laboratory Press; 1989.
28. Laborda J. 36B4 cDNA used as an estradiol-independent mRNA control is the cDNA for human acidic ribosomal phosphoprotein PO. *Nucl Acid Res*. 1991;19:3998.
29. Lyubarsky AL, Falsini B, Pennesi ME, Valentini P, Pugh EN. UV- and midwave-sensitive cone-driven retinal responses of the mouse: a possible phenotype for coexpression of cone photopigments. *J Neurosci*. 1999;19:442–455.

30. Liu Q, Lyubarsky A, Skalet JH, Pugh EN Jr, Pierce EA. RP1 is required for the correct stacking of outer segment discs. *Invest Ophthalmol Vis Sci*. 2003;44:4171–4183.
31. Westerfield M. *The Zebrafish Book: A Guide for the Laboratory Use of Zebrafish (Brachydanio rerio)*. Eugene, OR: University of Oregon Press; 1993.
32. Yee NS, Pack M. Zebrafish as a model for pancreatic cancer research. *Methods Mol Med*. 2005;103:273–298.
33. Jumaa H, Wei G, Nielsen PJ. Blastocyst formation is blocked in mouse embryos lacking the splicing factor SRp20. *Curr Biol*. 1999;9:899–902.
34. Xu X, Yang D, Ding JH, et al. ASF/SF2-regulated CaMKIIΔ alternative splicing temporally reprograms excitation-contraction coupling in cardiac muscle. *Cell*. 2005;120:59–72.
35. Wang HY, Xu X, Ding JH, Bermingham JR Jr, Fu XD. SC35 plays a role in T cell development and alternative splicing of CD45. *Mol Cell*. 2001;7:331–342.
36. Roshon MJ, Ruley HE. Hypomorphic mutation in hnRNP U results in post-implantation lethality. *Transgenic Res*. 2005;14:179–192.
37. Williamson DJ, Banik-Maiti S, DeGregori J, Ruley HE. hnRNP C is required for postimplantation mouse development but is dispensable for cell viability. *Mol Cell Biol*. 2000;20:4094–4105.
38. Kane DA, Kimmel CB. The zebrafish midblastula transition. *Development*. 1993;119:447–456.
39. Kane DA, Maischein HM, Brand M, et al. The zebrafish early arrest mutants. *Development*. 1996;123:57–66.
40. Wienholds E, Koudijs MJ, van Eeden FJ, Cuppen E, Plasterk RH. The microRNA-producing enzyme Dicer1 is essential for zebrafish development. *Nat Genet*. 2003;35:217–218.
41. Xu SY, Schwartz M, Rosenberg T, Gal A. A ninth locus (RP18) for autosomal dominant retinitis pigmentosa maps in the pericentromeric region of chromosome 1. *Hum Mol Genet*. 1996;5:1193–1197.
42. Takahashi N, Brooks HL, Wade JB, et al. Posttranscriptional compensation for heterozygous disruption of the kidney-specific NaK2Cl cotransporter gene. *J Am Soc Nephrol*. 2002;13:604–610.
43. Brissova M, Blaha M, Spear C, et al. Reduced PDX-1 expression impairs islet response to insulin resistance and worsens glucose homeostasis. *Am J Physiol Endocrinol Metab*. 2005;288:E707–E714.
44. Yuan L, Kawada M, Havlioglu N, Tang H, Wu JY. Mutations in PRPF31 inhibit pre-mRNA splicing of rhodopsin gene and cause apoptosis of retinal cells. *J Neurosci*. 2005;25:748–757.
45. Martinez-Gimeno M, Gamundi MJ, Hernan I, et al. Mutations in the pre-mRNA splicing-factor genes PRPF3, PRPF8, and PRPF31 in Spanish families with autosomal dominant retinitis pigmentosa. *Invest Ophthalmol Vis Sci*. 2003;44:2171–2177.
46. Tanaka T, Koizumi H, Gleeson JG. The doublecortin and doublecortin-like kinase 1 genes cooperate in murine hippocampal development. *Cereb Cortex*. 2006;16(suppl 1):i69–i73.
47. Young RW. The renewal of photoreceptor cell outer segments. *J Cell Biol*. 1967;33:61–72.
48. Young RW. The renewal of rod and cone outer segments in the rhesus monkey. *J Cell Biol*. 1971;49:303–318.
49. Nord AS, Chang PJ, Conklin BR, et al. The International Gene Trap Consortium Website: a portal to all publicly available gene trap cell lines in mouse. *Nucleic Acids Res*. 2006;34:D642–D648.
50. Parker LL, Gao J, Zuo J. Absence of hearing loss in a mouse model for DFNA17 and MYH9-related disease: the use of public gene-targeted ES cell resources. *Brain Res*. 2006;1091:235–242.
51. Gonzalez-Santos JM, Cao H, Wang A, et al. A complementation method for functional analysis of mammalian genes. *Nucleic Acids Res*. 2005;33:e94.
52. Comitato A, Spampanato C, Chakarova C, Sanges D, Bhattacharya SS, Marigo V. Mutations in splicing factor PRPF3, causing retinal degeneration, form detrimental aggregates in photoreceptor cells. *Hum Mol Genet*. 2007;16:1699–1707.